(IJUSE) 2015, Vol. No. 1, Jan-Dec **e-ISSN: 2454-759X, p-ISSN: 2454-7581**

A MATHEMATICAL STUDY OF BLOOD FLOW THROUGH STENOSED ARTERY

Sapna Ratan Shah
Department of Mathematics, Harcourt Butler Technological Institute, Kanpur - 208002, (India)

ABSTRACT

This paper deals with the rheological character of blood flow through stenosed artery by assuming blood as Bingham Plastic and Herschel-Bulkley fluid model. The irregularity of artery geometry is a frequent effect of vascular disease. Such constrictions disturb normal blood flow through the vessel. The results show that blood pressure increases very significantly in the upstream zone of the stenotic artery as the degree of the stenosis area severity increases. It is also shown that the non-Newtonian behaviour of blood has significant effects on the velocity profile of the blood flow and the magnitude of the wall shear stresses. It has been concluded in this paper that the Herschel-Bulkley fluid model is more realistic in comparison to Bingham Plastic fluid model. Present model is able to predict the main characteristics of the physiological flow of blood

Key words- *Bingham Plastic fluid model, Herschel-Bulkley fluid model, Apparent viscosity, Resistance to flow, Wall shear stress.*

1. INTRODUCTION

Arterial vessel trees perform the vital task of efficiently supplying blood to all organs and tissues of the body carrying nutrients and removing catabolic products. Hemodynamic simulation studies have been frequently used to gain a better understanding of functional, diagnostic and therapeutic aspects of blood flow. These simulations employed compartmental representations or branching tube models of arterial trees as their geometrical substrate, as well as localized multidimensional models have been often implemented to study arterial flow in more fine, detailed aspects. The study of the flow in the carotid artery bifurcation is of great clinical interest with respect to both, the genesis and the diagnostics of atherosclerotic diseases. It is well-known that the flow separation zone of the carotid sinus has the propensity to develop atherosclerotic plaques. In this sense, the local haemodynamic structure is intimately related to atherogenesis onset and progress. Consequently, a more deep understanding and better descriptions of the flow structure in that region would be of greatest importance to the early detection of stenoses (shown in Fig.1(a) and Fig.1(b)). Low shear stress regions are associated with the development of stenotics plaques. Despite the importance of chemical and physiological factors, the localized atherosclerotic lesions must be related to the local flow conditions as the other factor may be considered in a well mixed condition, i.e., uniformly distributed along the vessels. In the series of the papers, [Texon, (1); May et al., (2); Hershey and Cho, (3); Young, (4); Forrester and Young, (5); Caro et al., (6); Fry (7) Young and Tsai, (8); Lee, (9); Richard et al., (10)] the effects on the cardiovascular system can

be understood by studying the blood flow in its vicinity. In these studies the behavior of the blood has been considered as a Newtonian fluid. However, it may be noted that the blood does not behave as a Newtonian fluid under certain conditions. It is generally accepted that the blood, being a suspension of cells, behaves as a non-Newtonian fluid at low shear rate [Charm and Kurland, (11); Hershey et at., (12) Whitemore, (13); Cokelet, (14); Lih, (15); Shukla et al. (16)]. It has been pointed out that the flow behaviour of blood in a tube of small diameter (less than 0.2 mm) and at less than 20sec $^{-1}$ shear rate, can be represented by a

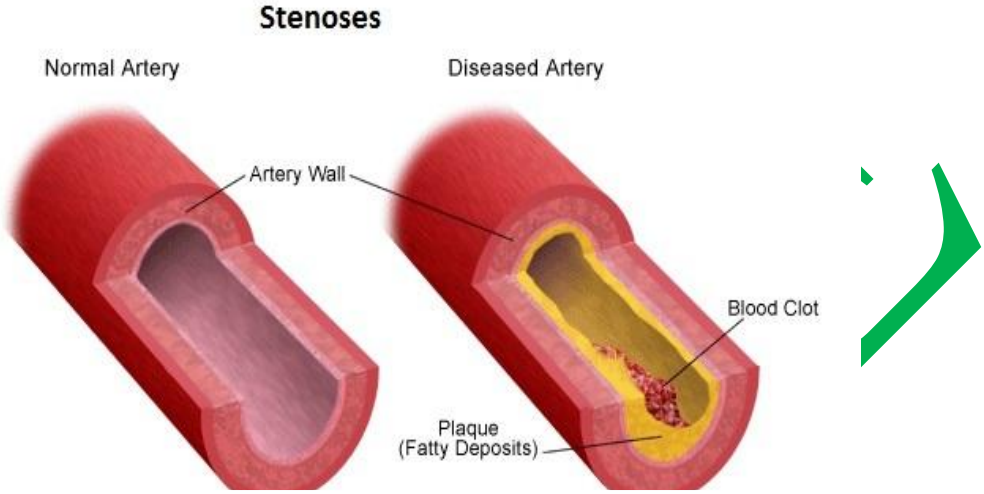

Fig.(1)a Fig.(1)b

power-low fluid [Hershey et al., (12); Charm et al., (11)]. It has also been suggested that at low shear rate (0.1 sec $^{-1}$) the blood exhibits yield stress and behaves like a Casson-model fluid [Casson, (17); Reiner and Scott-Blair, (18); Charm et al., (11)]. For blood flows in large arterial vessels (i.e., vessel diameter ≥1mm) [Labarbera, (19), Jung (23)], which can be considered as a large deformation flow, the predominant feature of the rheological behavior of blood is its shear rate dependent viscosity, and its fact on the hemodynamics of large arterial vessel flows has not been understood well. In this paper we investigated the effect of stenosis on the resistance to flow, apparent viscosity and wall shear stress in an artery by considering the blood as a Bingham Plastic fluid and Casson's-model fluids. And to examine the effect of stenosis shape parameter, we considered blood flow through an axially non-symmetrical but radially symmetric stenosis such that the axial shape of the stenosis can be change just by varying a parameter m.

2. FORMULATION OF THE PROBLEM

In the present analysis, it is assumed that the stenosis develops in the arterial wall in an axially non-symmetric but radially symmetric manner and depends upon the axial distance z and the height of its growth. In such a case the radius of artery, R(z) can be written as follows [Fig(2)]:

(IJUSE) 2015, Vol. No. 1, Jan-Dec **e-ISSN: 2454-759X, p-ISSN: 2454-7581**

$$\left.\begin{aligned}\frac{R(z)}{R_0} &= 1 - A[l_0^{(m-1)}(z-d) - (z-d)^m], && d \le z \le d + l_0 \\ &= 1, && \text{otherwise,}\end{aligned}\right\} \quad (1)$$

where R(z) and R_0 is the radius of the artery with and without stenosis, respectively. l_0 is the stenosis length and d indicates its location, $m \geq 2$ is a parameter determining the stenosis shape and is referred to as stenosis shape parameter. Axially symmetric stenosis occurs when m = 2, and a parameter A is given by;

$$A = \frac{\delta}{R_0 l_0^m} \frac{m^{m/(m-1)}}{(m-1)}$$

where δ_h denotes the maximum height of stenosis at $z = d + l_0 / m^{1/(m-1)}$. The ratio of the stenosis height to the radius of the normal artery is much less than unity.

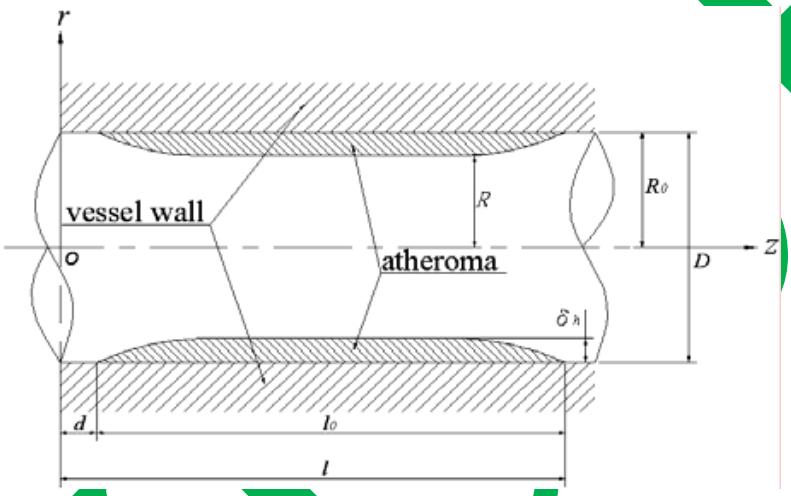

Fig (2). Geometry of Stenosis

2.1 Conservation equation and boundary condition:

The equation of motion for laminar and incompressible, steady, fully-developed, one-dimensional flow of blood whose viscosity varies along the radial direction in an artery reduces to [Young, (4)]:

$$\left.\begin{aligned}0 &= -\frac{\partial P}{\partial r} + \frac{1}{r}\frac{\partial (r\tau)}{\partial z}, \\ 0 &= -\frac{\partial P}{\partial r},\end{aligned}\right\} \quad (2)$$

where (z, r) are co-ordinates with z measured along the axis and r measured normal to the axis of the artery.

Following boundary conditions are introduced to solve the above equations,

$$\left.\begin{array}{ll} \partial u/\partial r = 0 & \text{at } r = 0 \\ u = 0 & \text{at } r = R(z) \\ \tau \text{ is finite} & \text{at } r = 0 \\ P = P_0 & \text{at } z = 0 \\ P = P_L & \text{at } z = l \end{array}\right\} \quad (3)$$

2.2 Bingham plastic fluid model:

The stress-strain relation is given by

$$\tau = \tau_0 + \mu\left(-\frac{du}{dr}\right) \quad (4)$$

where $\tau = \left(-\frac{dp}{dz}\frac{r}{2}\right)$, $\tau_0 = \left(-\frac{dp}{dz}\frac{R_P}{2}\right)$,

where u is axial viscosity, μ is viscosity of fluid and (–dp/dz) is pressure gradient.

2.3 Herschel-Bulkley fluid model:

The stress-strain relation of Herschel-Bulkley fluid is given as:

$$f(\tau) = \left(-\frac{du}{dr}\right) = \frac{1}{\mu}(\tau - \tau_0)^n, \qquad \tau \geq \tau_0$$

$$f(\tau) = \left(-\frac{du}{dr}\right) = 0, \qquad \tau \leq \tau_0 \quad (5)$$

where $\tau = \left(-\frac{dp}{dz}\frac{r}{2}\right)$, $\tau_0 = \left(-\frac{dp}{dz}\frac{R_c}{2}\right)$,

and μ denotes Herschel-Bulkley viscosity coefficient, τ_o is yield stress, τ is shear stress, R_c is the radius of the plug-flow region, u is the axial velocity along the z direction and n is the flow behavior index. The relation correspond to the vanishing of the velocity gradients in regions, in which the shear stress τ is less than the yield stress τ_o this implies a plug flow wherever $\tau \leq \tau_o$ when the shear rates in the fluid are very high, $\tau \geq \tau_o$, the power-law fluid behavior is indicated.

3. SOLUTION OF THE PROBLEM:

The expression for the velocity, u obtained as the solution of equation (2) subject to the boundary conditions (3) and equation (4), is obtained as (for $R_P \leq r \leq R(z)$)

$$u = \frac{R_0^2}{4\mu}\left(-\frac{dp}{dz}\right)((R/R_0)^2 - (r/R_0)^2) + (\tau_0 R_0/\mu)((R/R_0) - (r/R_0)) - (4R_0^{3/2}\tau_0/3\mu)\left(-\frac{1}{2\mu}\frac{dp}{dz}\right)^{1/2}((R/R_0)^{3/2} - (r/R_0)^{3/2}) \quad (6)$$

The constant plug flow velocity, u_P may be obtained from equation (5) evaluated at $r = R_P$.

The volumetric flow rate Q can be defined as,

$$Q = \int_0^R 2\pi u\, r\, dr = \pi \int_0^R r\left(-du/dr\right) dr, \tag{7}$$

The flow flux, Q when Rp<< R (i.e., the radius of the plug flow region is very small as compared to the non-plug flow region), is calculated as

$$Q = \frac{R_0^4 \pi}{8\mu}\left(-\frac{dp}{dz}\right)(R/R_0)^4 + -\frac{\tau_0 \pi}{3\mu}(R/R_0)^3 + -\frac{4R_0^{7/2}\pi}{7}\left\{\frac{\tau_0}{\mu^2}\frac{1}{2}\left(-\frac{dp}{dz}\right)(R/R_0)^7\right\}^{1/2} \tag{8}$$

$$Q = \frac{\pi R^4}{8\mu}\left(-\frac{dp}{dz}\right) f(\bar{y}), \tag{9}$$

From above equation pressure gradient is written as follows,

$$\left(-\frac{dp}{dz}\right) = \frac{8\mu Q}{\pi R_0^4} f(\bar{y}) \tag{10}$$

$$f(\bar{y}) = \left(\bar{y}\right)^4 + -\frac{\tau_0 \pi}{3\mu}\left(\bar{y}\right)^3 + -\frac{4R_0^{7/2}\pi}{7}\left\{\frac{\tau_0}{\mu}\left(-\frac{1}{2\mu}\frac{dp}{dz}\right)\left(\bar{y}\right)^7\right\}$$

Integrating equation (9) using the condition (3) $P = P_0$ at $z = 0$ and $P = P_l$ at $z = l$. We have

$$\Delta P = P_l - P_0 = \frac{8\mu Q}{\pi R_0^4}\int_0^l \frac{dz}{\left(R(z)/R_0\right)^4 f(\bar{y}(z))} \tag{11}$$

The resistance to flow is denoted by λ and defined as follows,

$$\lambda = \frac{P_l - P_0}{Q} \tag{12}$$

The resistance to flow from equation (11) using equations (10) is written as,

$$\lambda = 1 - \left(l_0/l\right) + \left(f_0/l\right)\int_d^{d+l_0} \frac{dz}{\left(R(z)/R_0\right)^4 f(\bar{y}(z))} \tag{13}$$

where f_0 is given by $f_0 = \left(R/R_0\right)^4 + -\frac{\tau_0 \pi}{3\mu}\left(R/R_0\right)^3 + -\frac{4R_0^{7/2}\pi}{7}\left\{\frac{\tau_0}{\mu}\left(-\frac{1}{2\mu}\frac{dp}{dz}\right)\left(R/R_0\right)^7\right\}$

Following the apparent viscosity (μ_{app}) is defined as follows;

$$\mu_{app} = \frac{1}{\left(R(z)/R_0\right)^4 f(\bar{y})} \tag{14}$$

The shearing stress at the wall can be defined as;

$$\tau_R = \tau_0 + \mu\left(-\frac{du}{dr}\right)_{r=R(z)} \tag{15}$$

By equation (1) and (5) we get,

$$\left(\frac{du}{dr}\right) = -\left(\frac{p}{2\mu}\right)^{1/n}\left[\left(r - R_c\right)^{1/n}\right], \tag{16}$$

the flow of flux, Q, is defined as,

$$Q=\int_0^R 2\,p\,u\,r\,dr = p\int_0^R r^2\left(-(du/dr)\right)dr, \tag{17}$$

substituting the value of $f(\tau)$ from equation (5) in equation (17),

$$Q = \frac{\pi}{2}\left(\frac{P}{2\mu}\right)^{1/n}\frac{R^{(3+\frac{1}{n})}}{(1+\frac{1}{n})}f(y), \tag{18}$$

where $f(y)=[2(1-\frac{R_c}{R})^{((1/n)+1)} - \frac{4}{((1/n)+2)}(1-\frac{R_c}{R})^{((1/n)+2)} + \frac{4}{((1/n)+2)((1/n)+3)}$

$((1-\frac{R_c}{R})^{((1/n)+3)} - ((-1)^{((1/n)+3)}(\frac{R_c}{R})))]$,

$\bar{y} = (R_c/R) << 1.$

Using equation (18) we have,

$$P = \left(-\frac{dp}{dz}\right) = \frac{2\mu}{R^{(1+3n)}}\left(\frac{2Q}{\pi f(\bar{y})}(1+\frac{1}{n})\right)^n \tag{19}$$

to determine λ, we integrate equation (19) for the pressure P_l and P_o are the pressure at z = 0 and z = *l*, respectively, where *l* is the length of the tube.

$$\Delta P = P_L - P_0 = \frac{2\mu}{\pi R_0^{1+3n}}\left(2Q\left(\frac{1}{n}+1\right)\right)^n \int_0^L \frac{dz}{(R(z)/R_0)^{(1+3n)}(f(\bar{y}))^n} \tag{20}$$

The resistance to flow is given by the coefficient λ is defined as follows:

$$\lambda = (P_l - P_0/Q) \tag{21}$$

$$\lambda_0 = \frac{2\mu}{R_0^{1+3n}}\left(\frac{2Q(1+\frac{1}{n})}{\pi}\right)^n (M) \tag{22}$$

$$M = \left(\int_0^d \frac{dz}{(f_0)^n} + \int_d^{d+l_0} \frac{dz}{\left(\frac{R(z)}{R_0}\right)^{1+3n}(f(\bar{y}))^n} + \int_{d+l_0}^{l} \frac{dz}{(f_0)^n}\right)$$

$$f_0 = \left[2\left(1-\bar{y}_1\right)^{(1+\frac{1}{n})} - \frac{4}{(\frac{1}{n}+2)}\left(1-\bar{y}_1\right)^{(2+\frac{1}{n})} + \frac{4}{(2+\frac{1}{n})(3+\frac{1}{n})}\left(\left(1-\bar{y}_1\right)^{(3+\frac{1}{n})} - \left((-1)^{(3+\frac{1}{n})}\bar{y}_1\right)\right)\right],$$

where $\bar{y}_1 = (R_c/R_0)$

When there is no stenosis in artery then $R = R_0$, the resistance to flow,

$$\lambda_N = \frac{2\mu}{R_0^{1+3n}}\left(\frac{2Q(1+\frac{1}{n})}{\pi}\right)^n \frac{L}{(f_0)^n} \tag{23}$$

from equation (22) and (23) the ratio of (λ / λ_N) is given as:

$$\lambda = \frac{\lambda_0}{\lambda_N} = 1 - \frac{l_0}{l} + \frac{(f_0)^n}{l}\int_d^{d+l_0} \frac{dz}{(R(z)/R_0)^{1+3n} f(\bar{y})^n} \tag{24}$$

The apparent viscosity (μ_0/μ) is defined as follow:

$$\mu_{app} = (1/(R(z)/R_0)^{1+3n} f(\bar{y}))$$

4. RESULTS AND DISCUSSION

In order to have estimate of the quantitative effects of various parameters involved in the analysis computer codes were developed and to evaluate the analytical results obtained for resistance to blood flow, apparent viscosity and wall shear stress for normal and diseased system associated with stenosis due to the local deposition of lipids have been determine.

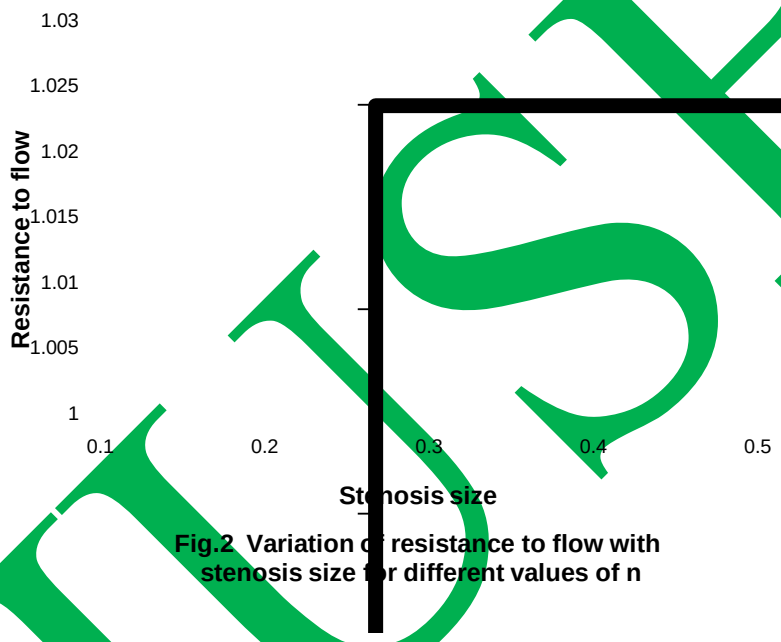

Fig.2 Variation of resistance to flow with stenosis size for different values of n

Fig.2 reveals the variation of resistance to flow (λ) with stenosis size (δ/R_0) for different values of flow behavior index (n). It is observed that the resistance to flow (λ) increases as stenosis size (δ/R_0) increases. It is also noticed here that resistance to flow (λ) increases as flow behavior index (n) increases. It is seen from the Fig.2, Fig.3 that the ratio is always greater than 1 and decreases as n decreases from unity. This result is similar with the result of [Shukla, et al., (16)]. In Fig.3, resistance to flow (λ) decreases as stenosis shape parameter (m) increases and maximum resistance to flow (λ) occurs at (m = 2), i. e. in case of symmetric stenosis. This result is therefore consisting to the result of [Haldar, (20)]. Fig.4 reveals the variation of apparent viscosity with stenosis shape parameter for different values of stenosis size. It may be observed here that the apparent viscosity decreases as stenosis shape parameter increases. This figure is also depicted that apparent viscosity decreases as stenosis size increases. In Fig.5 the variation of wall shear stress (τ) with stenosis length (l_0/l) for different values of flow behavior index (n) has been shown. This figure depicts that wall shear stress (τ) increases as stenosis length increases. Also it has been seen from this graph that the wall shear stress (τ) increases as value of flow behavior index (n) increases. As the stenosis grows, the wall shearing stress (τ) increases in the stenotic region. It is also noted that the shear ratio given by (15) is greater than one and decreases as n decreases (n <

(IJUSE) 2015, Vol. No. 1, Jan-Dec **e-ISSN: 2454-759X, p-ISSN: 2454-7581**

1). These results are similar with the results of [Shukla, et al., (16)]. It is also seen that the shear ratio is always greater than one and decreases as n decreases. For $\delta/R_0 = 0.1$ the increases in wall shear due to stenosis is about 37% when compared to the wall shear corresponding to the normal artery in the Newtonian case (n = 1), but for n = 2/3 this increase is only 23% approximately. However, for $\delta/R_0 = 0.2$, the corresponding increase in Newtonian (n = 1) and non-Newtonian (n = 2/3) cases are 95% and 56% respectively. Fig.6 consists the variation of resistance to flow (λ) with stenosis size (δ/R_o) for different values of stenosis shape parameter (m). It is observed here that the resistance to flow increases as stenosis size increases. It should be also noted here that the resistance to flow decreases as stenosis shape parameter (m) increases. These results are therefore consistent with the observation of [Haldar, (20)].

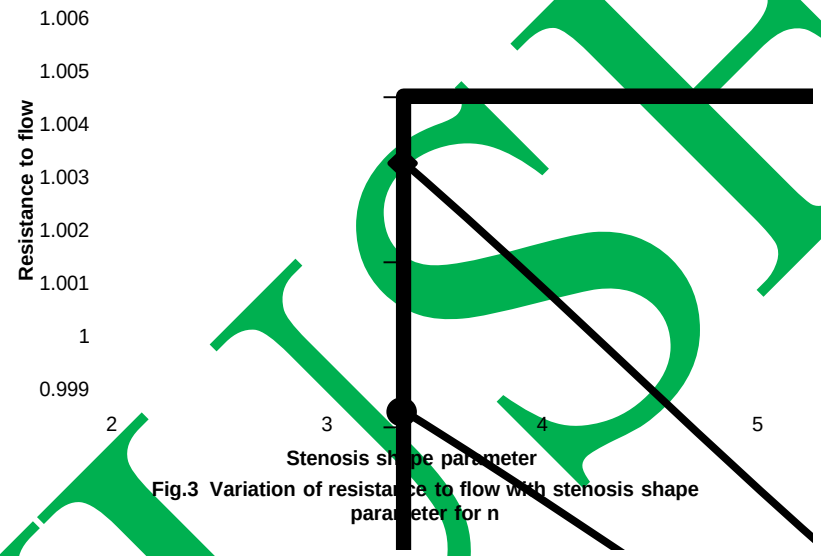

Fig.3 Variation of resistance to flow with stenosis shape parameter for n

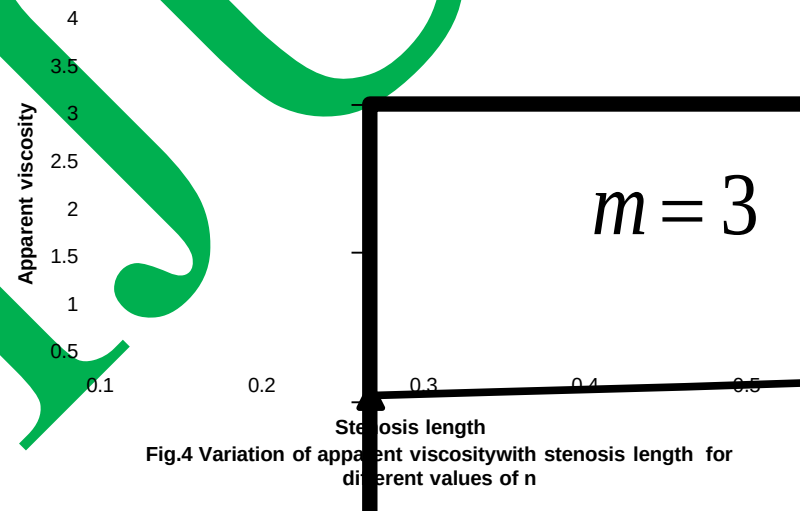

Fig.4 Variation of apparent viscositywith stenosis length for different values of n

Fig.7 reveals the variation of apparent viscosity (μ_o/μ) with stenosis size (δ/R_o) for different values of. stenosis shape parameter (m). It may be observed here that the apparent viscosity decreases as shape parameter of stenosis increases. This figure is also depicted that apparent viscosity increases as stenosis size increases. In an artery flow, the viscosity of blood found to vary with the arterial radius decreasing with it. The diabetic patients are more prone to the various cardiovascular

(IJUSE) 2015, Vol. No. 1, Jan-Dec **e-ISSN: 2454-759X, p-ISSN: 2454-7581**

diseases. The viscosity of the diabetic patients is higher than that of normal. Therefore the blood viscosity of diabetic patients is lowered by regular dose of aspirin or injecting saline water in order to dilute the blood. This lowers the blood pressure. Fig.8 describes the variation of wall shear stress with stenosis sise for different values of stenosis shape parameter (m). In this graph, wall shear stress increases as stenosis size increases. This result is obvious because the lumen radius decreases as stenosis size increases. It is also noticed here that wall shear stress decreases as stenosis shape parameter increases. This result is similar with the result of [Pontrelli, (21)].

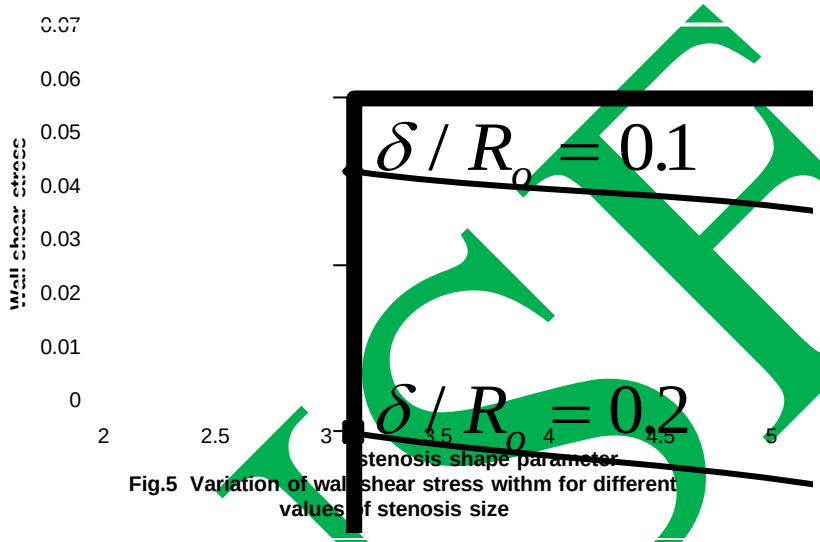

Fig.5 Variation of wall shear stress withm for different values of stenosis size

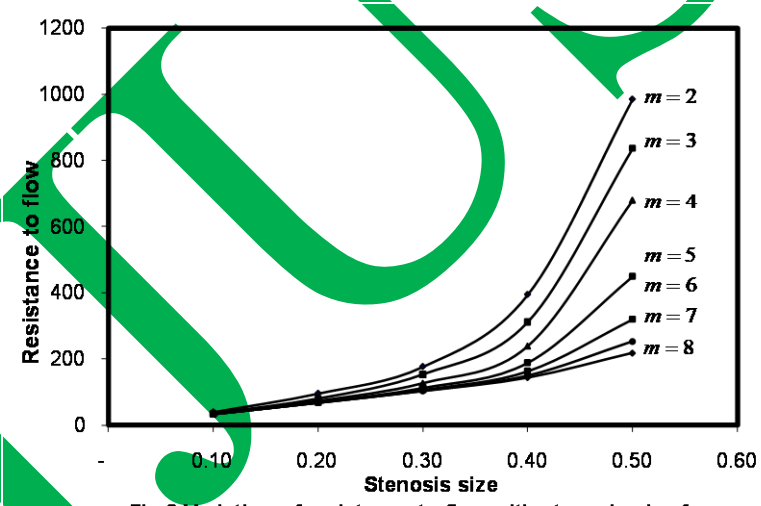

Fig.6 Variation of resistance to flow with stenosis size for different values of shape parameter

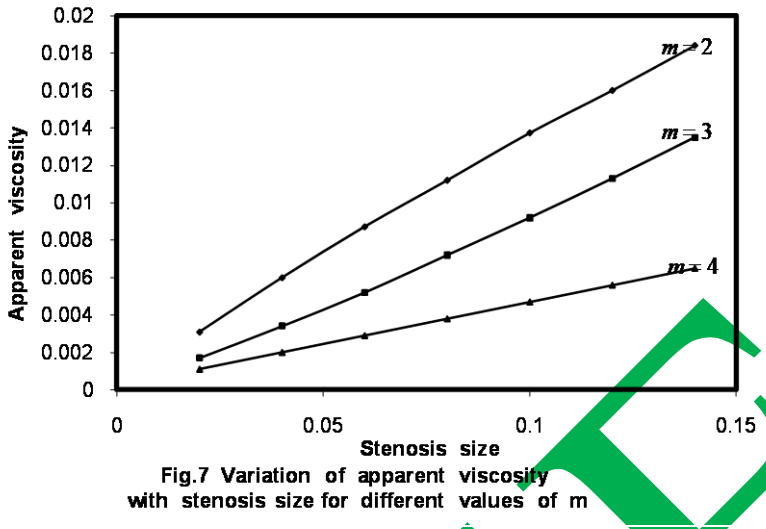

Fig.7 Variation of apparent viscosity with stenosis size for different values of m

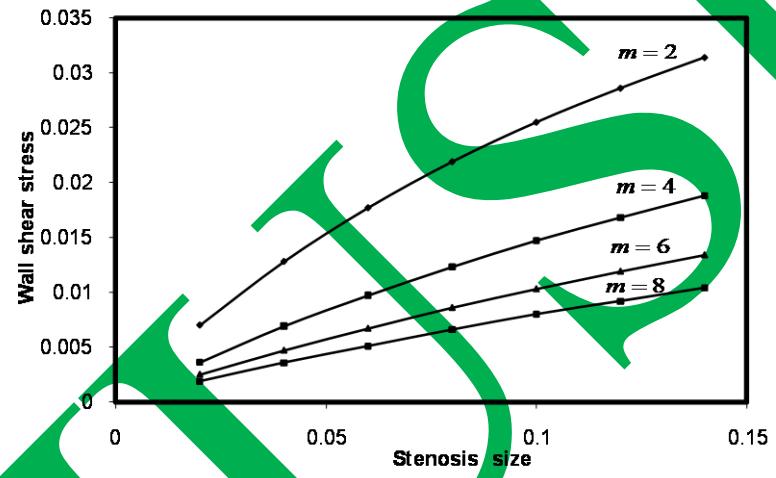

Fig.8 Variation of wall shear stress with stenosis size for different values of m

5. CONCLUSION

In this paper, we have compare the results for both models. studied the effects of the stenosis in an artery by considering the blood as Bingham Plastic and Herschel-Bulkley fluid model. It has been concluded that the resistance to flow and wall shear stress increases as the size of stenosis increases for a given non-Newtonian model of the blood. These increases are however, small due to non-Newtonian behaviour of the blood. It is noted that the non-Newtonian behaviour only slightly affects the pressure distribution. The results also indicate that as the degree of the stenosis area severity increases, the pressure gradient required to impel the blood passing through the narrowing channel increases significantly. This results in a higher pressure to occur in the up-stream region. The results clearly show how blood pressure increases as the degree of the stenosis severity increases. The non-Newtonian behaviour has very significant effect on the magnitude of wall shear stresses.

REFERENCES

1. Texon, M., A homodynamic concept of atherosclerosis with particular reference to coronary occlusion. 99. 418: (1957).
2. May, A. G., Deweese, J. A. and Rob, C. B., Hemodynamic effects of arterial stenosis. Surgery, 53: 513-524. (1963).
3. Hershey, D., Cho, S. J., Blood flow in ridig tubes: Thickness and slip velocity of plasma film at the wall. J. Appli. Physiolo.21:27. (1966).
4. Young, D. F., Effects of a time-dependent stenosis on flow through a tube. J. Eng. India. Trans. ASME. 90: 248-254. (1968).
5. Forrester, J. H. and Young, D. F., Flow through a converging diverging tube and its implications in occlusive vascular disease. J. Biomech. 3: 297-316. (1970).
6. Caro, C. G., Fitz-Gerald J. M., and Schroter R. C., Atheroma and arterial wall shear observation, Correlation and proposal of a shear dependent mass transfer mechanism for Atherogenesis. Proc. R. Soc. 177: 109-159. (1971).
7. Fry, D. L., Localizing factor in arteriosclerosis, In atherosclerosis and coronary heart disease, NewYork: Grune Stratton. 85, (1972)
8. Young, D. F. and Tsai, F. Y., Flow characteristics in models of arterial stenosis–II, unsteady flow. J. Biomech. 6: 547-558. (1973).
9. Lee, J. S., On the coupling and detection of motion between an artery with a localized lesion and its surrounding tissue. J. Biomech. 7: 403. (1974).
10. Richard, L. K., Young, D. F. and Chalvin, N. R., Wall vibrations induced by flow through simulated stenosis in models and arteries. J. Biomech. 10: 431. (1977).
11. Charm, S. E., and Kurland G. S., Viscometry of human blood for shear rate of 100,000sec^{-1}. Nature London. 206: 617-618. (1965).
12. Hershey, D., Byrnes, R. E., Deddens, R. L. and Roa. A. M., Blood rheology: Temperature dependence of the power law model. Paper presented at A.I.Ch.E. Boston (1964).
13. Whitmore R. L., Rheology of the circulation, Perg NewYork (1968).
14. Cokelet, G. R., The rheology of human blood. In Biomechanics, Ed. By Y. C. Fung et al., 63, Englewood Cliffs: Prentice-Hall, (1972).
15. Lih, M.M, Transport Phenomena in Medicine and Biology. Wiley, New York, (1975).
16. Shukla, J. B., Parihar, R. S., Gupta, S. P.,Biorheological aspects of blood flow through artery with mild stenosis:Effects of peripheral layer.Biorhe.17:403-410. (1990).
17. Casson, N. A flow equation for pigment oil suspensions of the printing ink type. In Rheology of disperse systems, Ed. Mill., C.C., London. 84-102. (1959).
18. Reiner, M. and Scott Baldair G.W., The flow of the blood through narrow tube. Nature, London, 184: 354-359, (1959).
19. Labarbera, M., Principles of design of fluid transport systems in zoology. Science. 249: 992-1000. (1997).
20. K. Haldar, Effects of the shape of stenosis on the resistance to blood flow through an artery. Bull. Mathe. Bio. 47: 545-550. (1985).

21. Pontrelli, G., "Blood flow through an axisymmetric stenosis", Proc. Inst Mech. Eng, Part H, Eng Med., 215: 1-10. (2013).
22. Tandon, P. N., Nirmala, P., Tewari, M. and Rana, U. S., Analysis of nutritional transport through a capillary: Normal and stenosed. Compu. Math. Appli. 22. 12: 3-13, (1991).
23. Jung, H., Choil, J. W. and Park, C. G., (2011) "Asymmetric flows of non-Newtonian fluids in symmetric stenosis artey" Vol. 16, 2 june pp. 101-108.